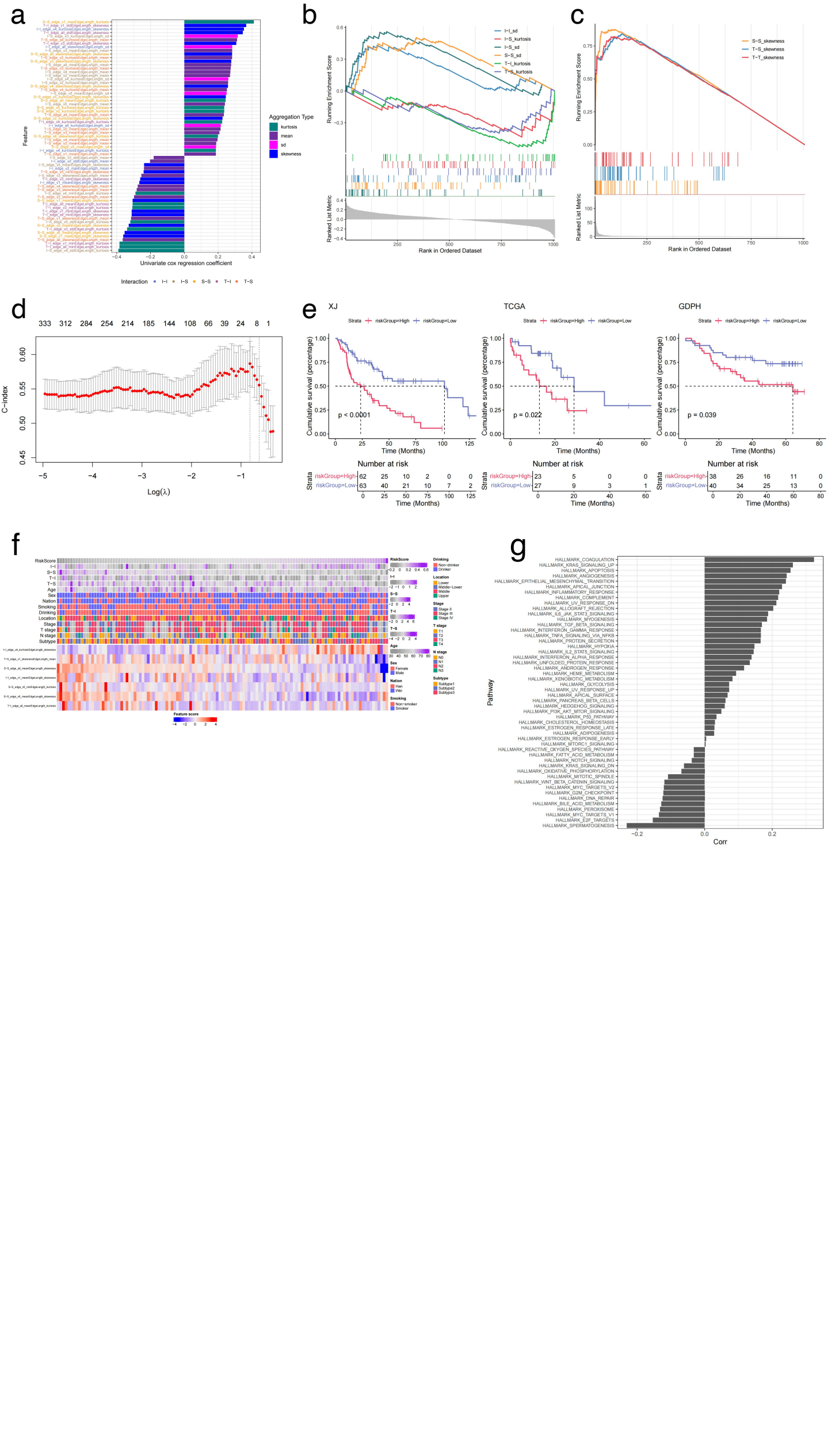
a
Feature
Univariate cox regression coefficient
Aggregation Type
kurtosis
mean
sd
skewness
Interaction
I–I
I–S
S–S
T–I
T–S
b
Running Enrichment Score
I–I_sd
I–S_kurtosis
I–S_sd
S–S_sd
T–I_kurtosis
T–S_kurtosis
Ranked List Metric
Rank in Ordered Dataset
c
Running Enrichment Score
S–S_skewness
T–S_skewness
T–T_skewness
Ranked List Metric
Rank in Ordered Dataset
d
333 312 284 254 214 185 144 108 66 39 24 8 1
C-index
Log(λ)
e
XJ
TCGA
GDPH
Strata
riskGroup=High
riskGroup=Low
Cumulative survival (percentage)
p < 0.0001
p = 0.022
p = 0.039
Time (Months)
Number at risk
riskGroup=High 62 25 10 2 0 0
riskGroup=Low 63 40 21 10 7 2
riskGroup=High 23 5 0 0
riskGroup=Low 27 9 3 1
riskGroup=High 38 26 16 11 0
riskGroup=Low 40 34 25 13 0
f
RiskScore
I–I
S–S
T–I
T–S
Age
Sex
Nation
Smoking
Drinking
Location
Stage
T stage
N stage
Subtype
Feature score
Drinking
Non-drinker
Drinker
Location
Lower
Middle–Lower
Middle
Upper
Stage
Stage II
Stage III
Stage IV
T stage
T1
T2
T3
T4
N stage
N0
N1
N2
N3
Subtype
Subtype1
Subtype2
Subtype3
Sex
Female
Male
Nation
Han
Wei
Smoking
Non–smoker
Smoker
g
Pathway
HALLMARK_COAGULATION
HALLMARK_KRAS_SIGNALING_UP
HALLMARK_APOPTOSIS
HALLMARK_ANGIOGENESIS
HALLMARK_EPITHELIAL_MESENCHYMAL_TRANSITION
HALLMARK_APICAL_JUNCTION
HALLMARK_INFLAMMATORY_RESPONSE
HALLMARK_COMPLEMENT
HALLMARK_UV_RESPONSE_DN
HALLMARK_ALLOGRAFT_REJECTION
HALLMARK_IL6_JAK_STAT3_SIGNALING
HALLMARK_MYOGENESIS
HALLMARK_TGF_BETA_SIGNALING
HALLMARK_INTERFERON_GAMMA_RESPONSE
HALLMARK_TNFA_SIGNALING_VIA_NFKB
HALLMARK_PROTEIN_SECRETION
HALLMARK_HYPOXIA
HALLMARK_IL2_STAT5_SIGNALING
HALLMARK_INTERFERON_ALPHA_RESPONSE
HALLMARK_UNFOLDED_PROTEIN_RESPONSE
HALLMARK_ANDROGEN_RESPONSE
HALLMARK_HEME_METABOLISM
HALLMARK_XENOBIOTIC_METABOLISM
HALLMARK_GLYCOLYSIS
HALLMARK_UV_RESPONSE_UP
HALLMARK_APICAL_SURFACE
HALLMARK_PANCREAS_BETA_CELLS
HALLMARK_HEDGEHOG_SIGNALING
HALLMARK_PI3K_AKT_MTOR_SIGNALING
HALLMARK_P53_PATHWAY
HALLMARK_CHOLESTEROL_HOMEOSTASIS
HALLMARK_ESTROGEN_RESPONSE_LATE
HALLMARK_ADIPOGENESIS
HALLMARK_ESTROGEN_RESPONSE_EARLY
HALLMARK_MTORC1_SIGNALING
HALLMARK_REACTIVE_OXYGEN_SPECIES_PATHWAY
HALLMARK_FATTY_ACID_METABOLISM
HALLMARK_NOTCH_SIGNALING
HALLMARK_KRAS_SIGNALING_DN
HALLMARK_OXIDATIVE_PHOSPHORYLATION
HALLMARK_MITOTIC_SPINDLE
HALLMARK_WNT_BETA_CATENIN_SIGNALING
HALLMARK_MYC_TARGETS_V2
HALLMARK_G2M_CHECKPOINT
HALLMARK_DNA_REPAIR
HALLMARK_BILE_ACID_METABOLISM
HALLMARK_PEROXISOME
HALLMARK_MYC_TARGETS_V1
HALLMARK_E2F_TARGETS
HALLMARK_SPERMATOGENESIS
Corr

Figure S1. Prognostic risk stratification based on pathological features.
(a) Bar plot of significant prognostic features (univariate cox *p*-value < 0.05), color-coded by aggregation method (bars) and feature type (y-axis). (b) Enrichment analysis of feature risk scores. (c) Enrichment analysis of feature variable coefficients. (d) Concordance index (C-index) trajectories during five-fold cross-validation. (e) Kaplan-Meier survival curves demonstrating model performance across three independent cohorts. (f) Heatmap displaying model-used features with aligned clinical annotations. (g) Correlation analysis between model risk scores and Hallmark pathway GSVA values, presented as a ranked bar plot.

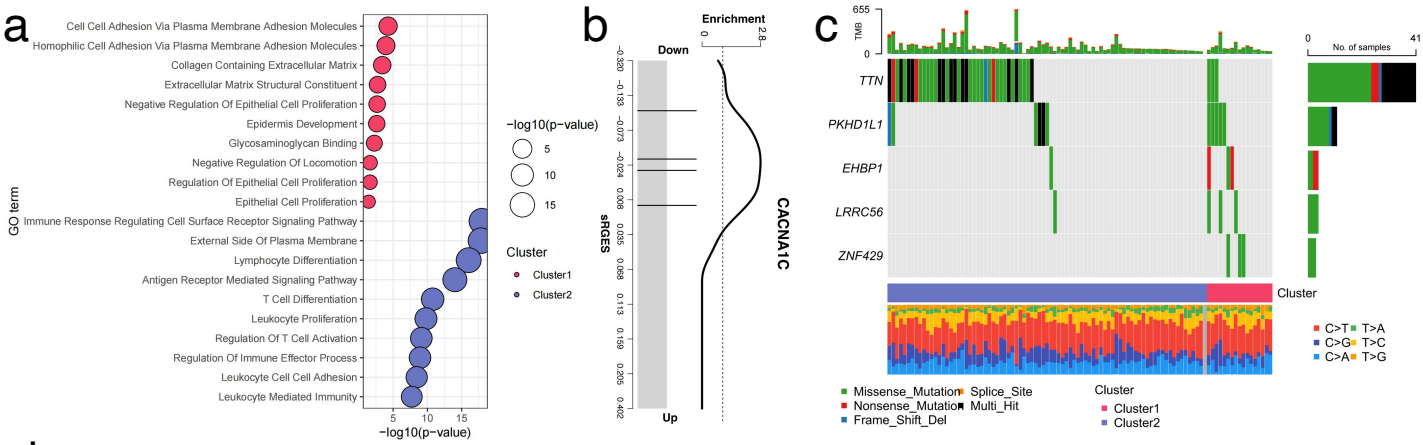

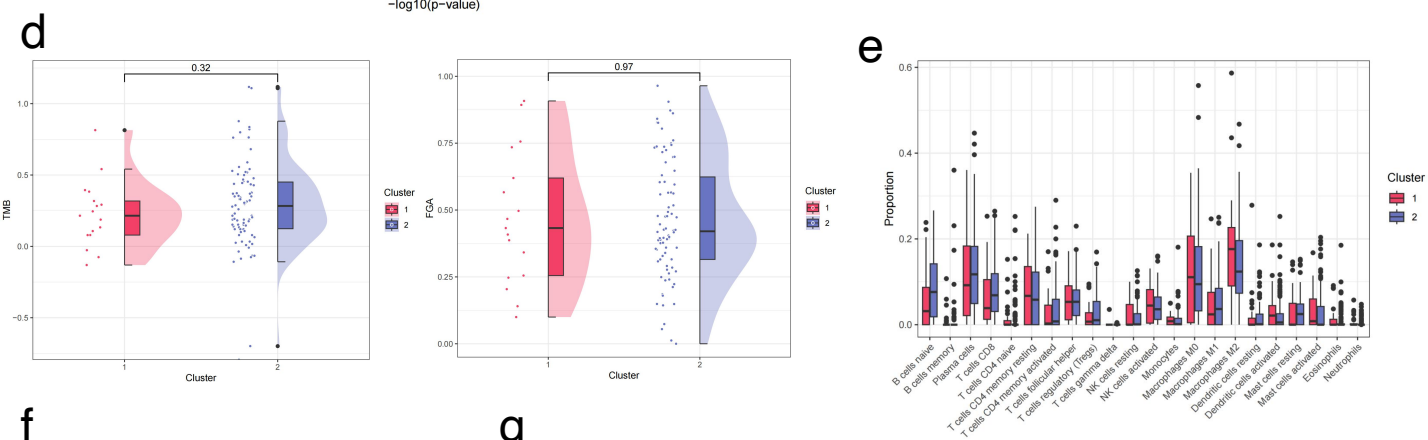

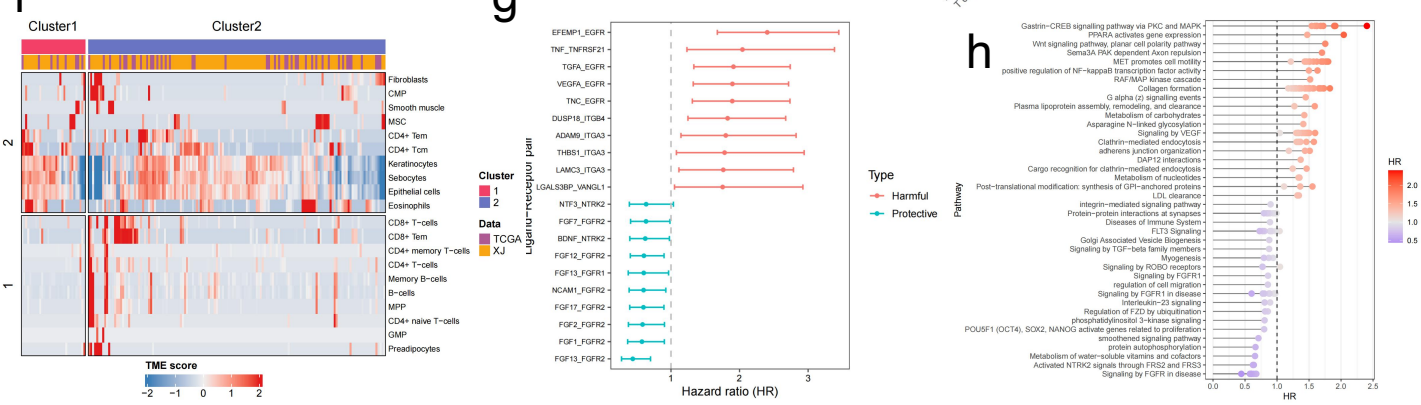

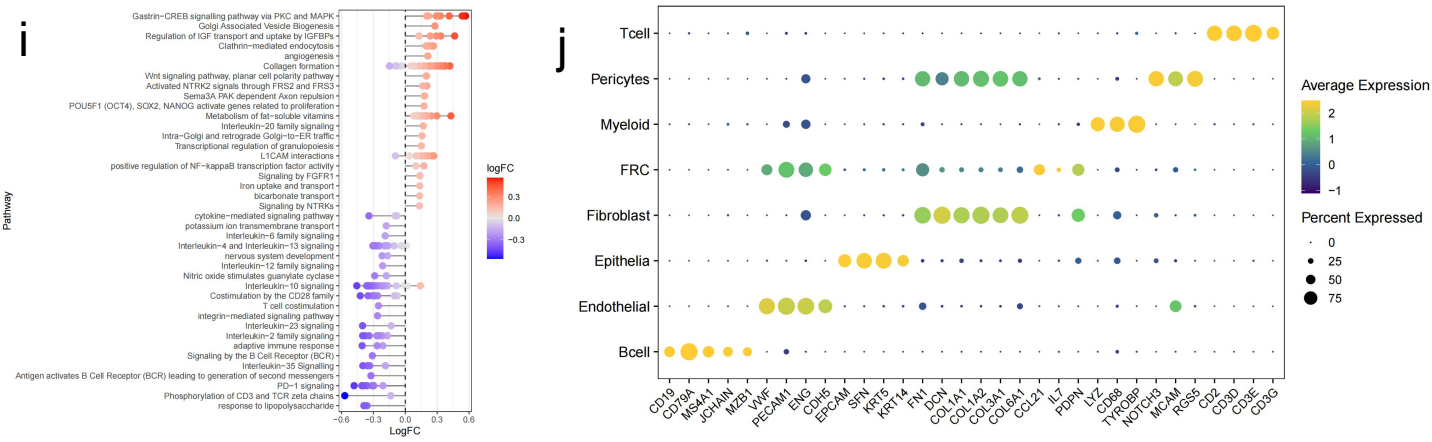

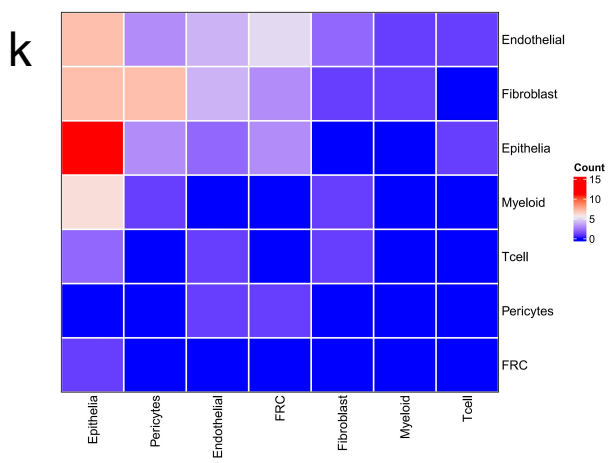

m

Cell	Receptor_count	Ligand_count
Mes	15	16
Pericytes	13	2
FRC	11	1
QP	10	1
AP	7	1
TEC4	5	2
TEC5	4	NA
CAF4	3	8
TEC2	2	7
NMF	1	8
Mono01	1	3
Mono03	1	1
TN	1	NA
CAF1	1	NA
NK/NKT	1	NA
TEC3	NA	8
CAF2	NA	6
TMEM−CD4	NA	3
Mucosal	NA	2
Mast	NA	1
NEC1	NA	1
TEX	NA	1
Pericyte	NA	1
TAM02	NA	1
TAM01	NA	1
TAM03	NA	1

l

Cell	Receptor_count	Ligand_count
Epithelia	34	20
Pericytes	14	2
Endothelial	12	23
FRC	12	1
Fibroblast	5	23
Myeloid	2	8
Tcell	2	4

Figure S2. Molecular dynamics of prognostic risk stratification in esophageal squamous cell carcinoma (ESCC).

(a) ORA using GOBP terms, showing the top 10 up- and down-regulated terms. (b) CACNA1C enriched profile. (c) Significantly mutated genes between pathological subtypes. (d) Tumor mutational burden and fraction of genome altered values across pathological subtypes. (e-f) Cell abundance of pathological subtypes predicated by Cibersort and xCell. (g) Forest plot of significant prognostic receptor-ligand pairs, showing the top 10 protective and hazardous pairs. (h-i) Hazard ratio (HR) and LogFC distribution of receptor-ligand pairs in pathway contexts. (j) Canonical markers for major cell types. (k) Heatmap mapping receptor-ligand pairs to their predominant cellular sources. (l-m) Cellular localization frequency counts for receptor-ligand pairs at major cell type and subtypes resolution.

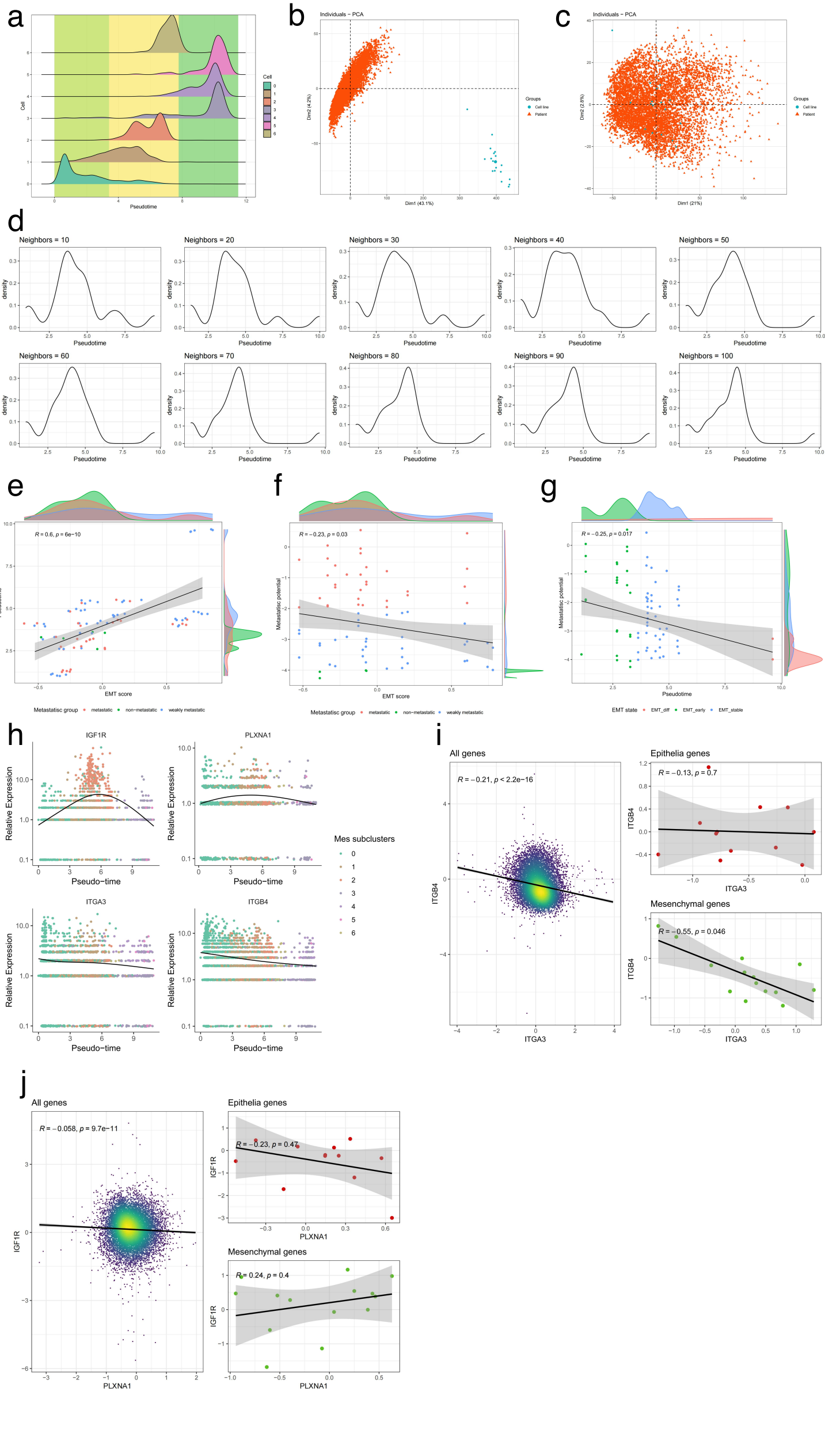
a
Cell
Pseudotime
b
Individuals − PCA
Dim2 (4.2%)
Dim1 (43.1%)
Groups
Cell line
Patient
c
Individuals − PCA
Dim2 (2.8%)
Dim1 (21%)
Groups
Cell line
Patient
d
Neighbors = 10
Neighbors = 20
Neighbors = 30
Neighbors = 40
Neighbors = 50
Neighbors = 60
Neighbors = 70
Neighbors = 80
Neighbors = 90
Neighbors = 100
density
Pseudotime
e
R = 0.6, p = 6e−10
Pseudotime
EMT score
Metastatisc group
metastatic
non−metastatic
weakly metastatic
f
R = −0.23, p = 0.03
Metastatisc potential
EMT score
Metastatisc group
metastatic
non−metastatic
weakly metastatic
g
R = −0.25, p = 0.017
Metastatisc potential
Pseudotime
EMT state
EMT_diff
EMT_early
EMT_stable
h
IGF1R
PLXNA1
ITGA3
ITGB4
Relative Expression
Pseudo−time
Mes subclusters
0
1
2
3
4
5
6
i
All genes
R = −0.21, p < 2.2e−16
ITGB4
ITGA3
Epithelia genes
R = −0.13, p = 0.7
ITGB4
ITGA3
Mesenchymal genes
R = −0.55, p = 0.046
ITGB4
ITGA3
j
All genes
R = −0.058, p = 9.7e−11
IGF1R
PLXNA1
Epithelia genes
R = −0.23, p = 0.47
IGF1R
PLXNA1
Mesenchymal genes
R = 0.24, p = 0.4
IGF1R
PLXNA1

Figure S3. Validation of epithelial-to-mesenchymal transition (EMT) trajectories. (a) Pseudo-time score distribution across MESs. (b-c) PCA of integrated cell line and single-cell data before and after batch effect correction. (d) Pseudo-time score distribution under varying KNN parameters. (e-g) Correlation analyses between: EMT score and pseudo-time, EMT score and metastatic potential, and pseudo-time and metastatic potential. (h) State-specific expression patterns of MES-specific receptors. (i-j) Knockdown signature correlation between: *ITGA3* and *ITGB4*, *IGF1R* and *PLXNA1*.

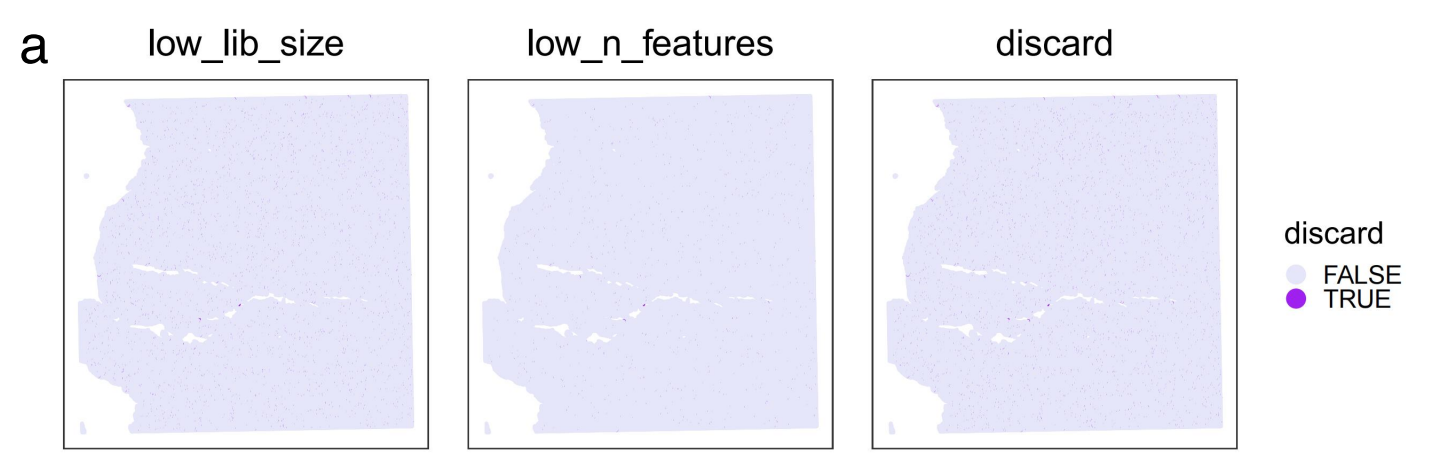
a
low_lib_size
low_n_features
discard
discard
FALSE
TRUE


b
Type
ITGA3−ITGB4−
ITGA3−ITGB4+
ITGA3+ITGB4−
ITGA3+ITGB4+

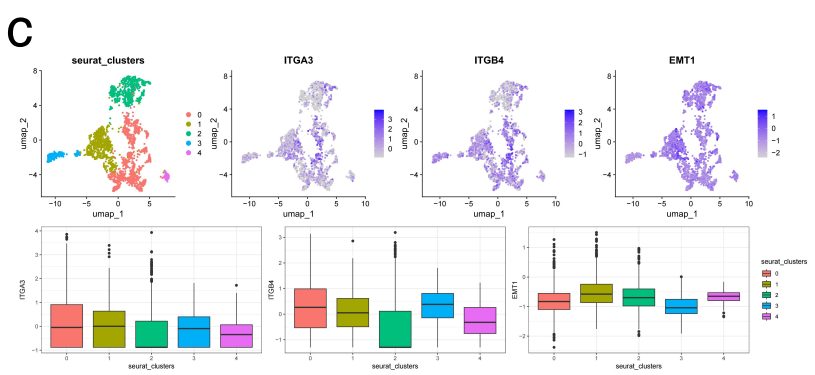
c
seurat_clusters
ITGA3
ITGB4
EMT1
umap_1
umap_2
seurat_clusters

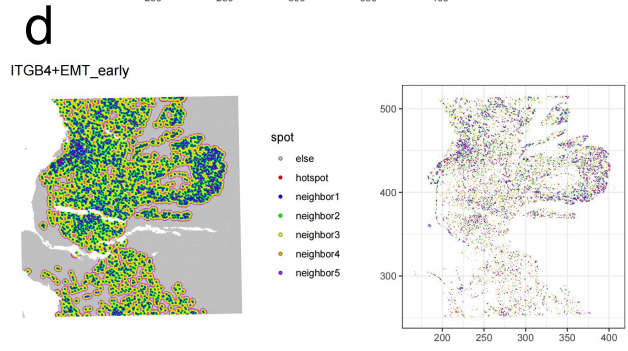
d
ITGB4+EMT_early
spot
else
hotspot
neighbor1
neighbor2
neighbor3
neighbor4
neighbor5

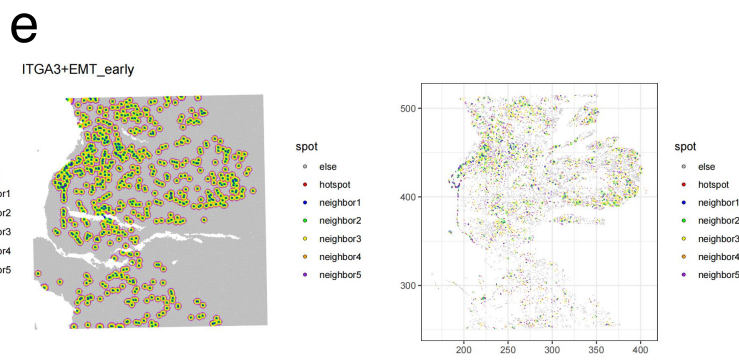
e
ITGA3+EMT_early
spot
else
hotspot
neighbor1
neighbor2
neighbor3
neighbor4
neighbor5

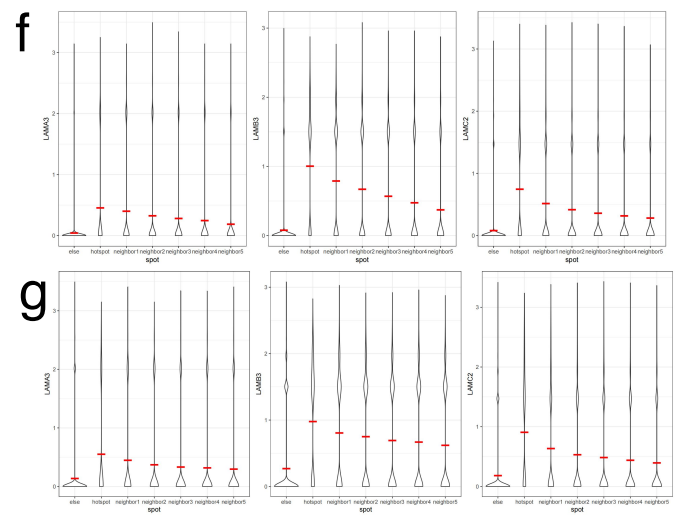
f
LAMA3
LAMB3
LAMC2
spot

g
LAMA3
LAMB3
LAMC2
spot

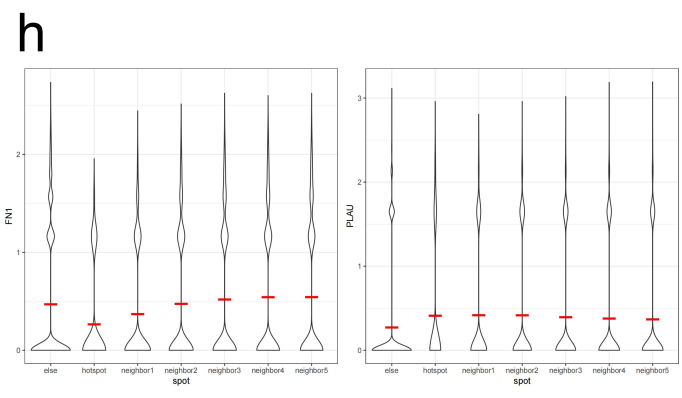
h
FN1
PLAU
else
hotspot
neighbor1
neighbor2
neighbor3
neighbor4
neighbor5
spot

Figure S4.Quality control and co-localization in Visium HD data.
(a) Quality-control metrics for the Visium HD data. Spots with low library size and low number of detected unique features were discarded. (b) Spatial mapping of EMT-early across the tissue section. (c) UMAP visualization and box plot of EMT-early. (d) ITGB4^{+} EMT-early with their neighbors in all spots and in EMT-early spots. (e) ITGA3^{+} EMT-early with their neighbors in all spots and in EMT-early spots. (f) Co-localization of ITGB4^{+} EMT-early with their autocrine ligand. (g) Co-localization of ITGA3^{+} EMT-early with their autocrine ligand. (h) Co-localization of ITGA3^{+} EMT-early with CAF4-specific ligands.

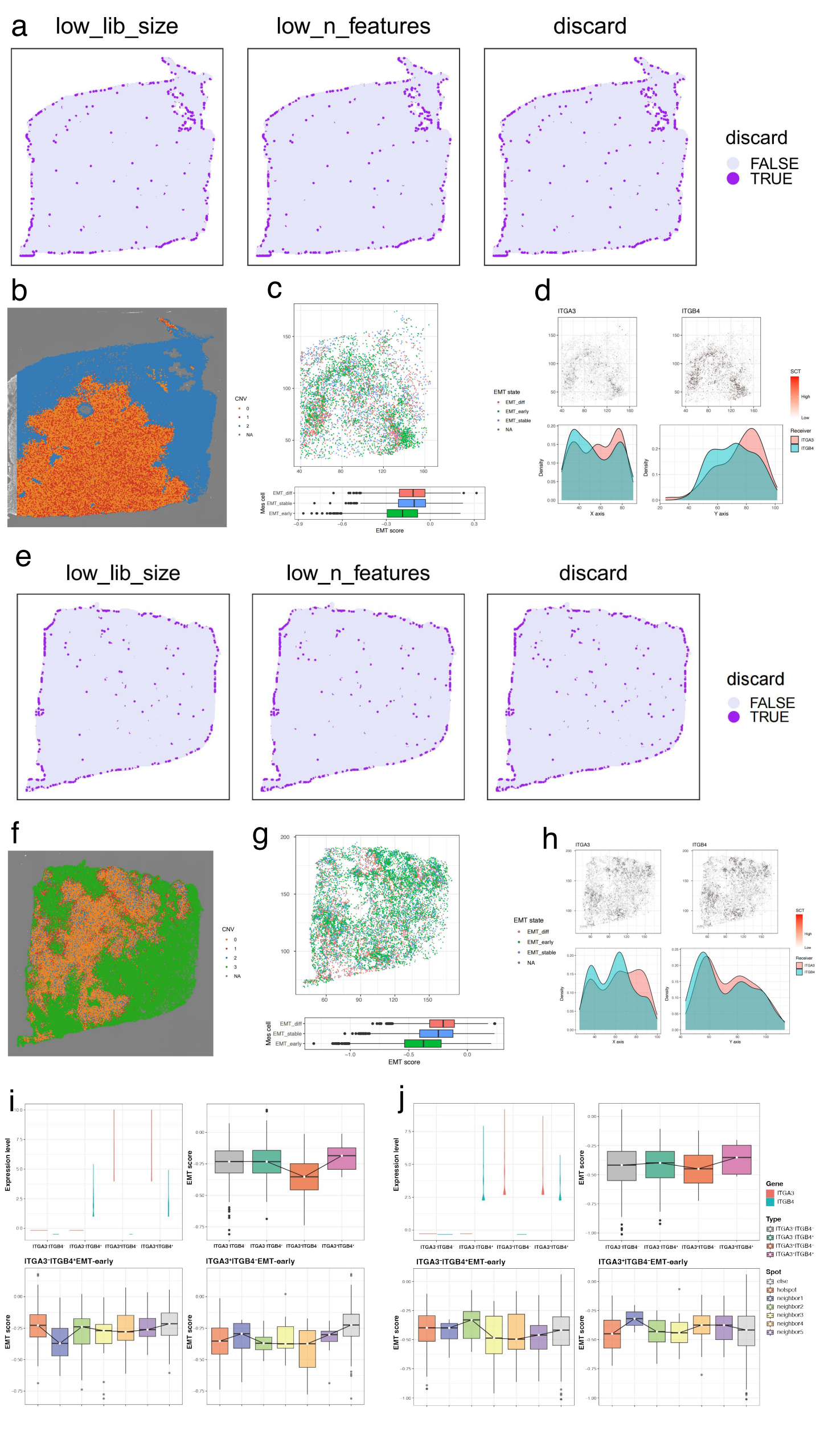
a
low_lib_size
low_n_features
discard
discard
FALSE
TRUE
b
c
CNV
0
1
2
NA
EMT_diff
EMT_stable
EMT_early
Mes cell
EMT score
d
ITGA3
ITGB4
EMT state
EMT_diff
EMT_early
EMT_stable
NA
SCT
High
Low
Receiver
ITGA3
ITGB4
Density
X axis
Y axis
e
low_lib_size
low_n_features
discard
discard
FALSE
TRUE
f
CNV
0
1
2
3
NA
g
EMT_diff
EMT_stable
EMT_early
Mes cell
EMT score
h
ITGA3
ITGB4
EMT state
EMT_diff
EMT_early
EMT_stable
NA
SCT
High
Low
Receiver
ITGA3
ITGB4
Density
X axis
Y axis
i
Expression level
EMT score
ITGA3⁻ITGB4⁻
ITGA3⁻ITGB4⁺
ITGA3⁺ITGB4⁻
ITGA3⁺ITGB4⁺
ITGA3⁻ITGB4⁺EMT-early
ITGA3⁺ITGB4⁻EMT-early
j
Expression level
EMT score
Gene
ITGA3
ITGB4
Type
ITGA3⁻ITGB4⁻
ITGA3⁻ITGB4⁺
ITGA3⁺ITGB4⁻
ITGA3⁺ITGB4⁺
ITGA3⁻ITGB4⁺EMT-early
ITGA3⁺ITGB4⁻EMT-early
Spot
else
hotspot
neighbor1
neighbor2
neighbor3
neighbor4
neighbor5

Figure S5. Quality control and co-localization in Stereo-seq data.
(a, e) Quality-control metrics for the Stereo-seq data in E1 and E2 samples. (b, f) CNA inference results. (c, g) Spatial mapping of EMT states. (d, h) Spatial visualization of *ITGA3* and *ITGB4*. (i, j) Spatial correlation between *ITGA3/ITGB4*-specific EMT-*early* spots and regional EMT activity

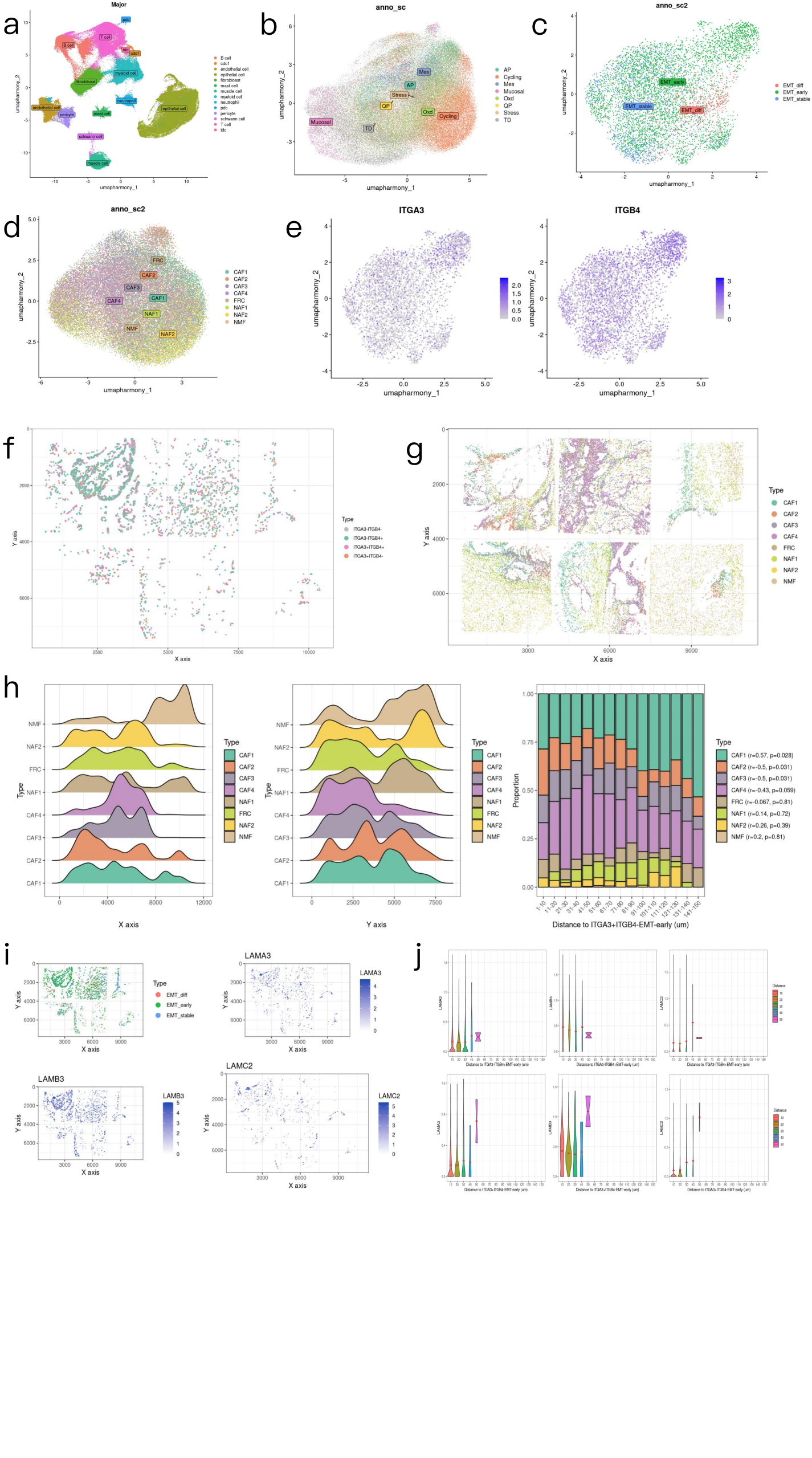
a
Major
pdc
T cell
B cell
tdc
cdc1
myeloid cell
fibrobloast
mast cell
neutrophil
endothelial cell
pericyte
epithelial cell
schwann cell
muscle cell
umapharmony_1
umapharmony_2
b
anno_sc
Mes
AP
Stress
QP
Oxd
Cycling
Mucosal
TD
c
anno_sc2
EMT_early
EMT_stable
EMT_diff
d
anno_sc2
FRC
CAF2
CAF3
CAF4
CAF1
NAF1
NMF
NAF2
e
ITGA3
ITGB4
f
Type
ITGA3-ITGB4-
ITGA3-ITGB4+
ITGA3+ITGB4+
ITGA3+ITGB4-
X axis
Y axis
g
h
Type
CAF1
CAF2
CAF3
CAF4
NAF1
FRC
NAF2
NMF
X axis
Y axis
Proportion
Distance to ITGA3+ITGB4-EMT-early (um)
CAF1 (r=0.57, p=0.028)
CAF2 (r=-0.5, p=0.031)
CAF3 (r=-0.5, p=0.031)
CAF4 (r=-0.43, p=0.059)
FRC (r=-0.067, p=0.81)
NAF1 (r=0.14, p=0.72)
NAF2 (r=0.26, p=0.39)
NMF (r=0.2, p=0.81)
i
Type
EMT_diff
EMT_early
EMT_stable
LAMA3
LAMB3
LAMC2
X axis
Y axis
j
Distance
Distance to ITGA3-ITGB4+EMT-early (um)

Figure S6. Co-localization in Xenium data.

(a) Major cell annotations of Xenium data. (b-d) Cell subtype annotations of Epithelial cells, Mes cells, and Fibroblasts. (e) *ITGA3* and *ITGB4* expression distribution in Mes cells. (f-g) Mes and Fibroblast subtype in situ distribution. (h) Left and Middle, Kernel density plots displaying the Fibroblast distribution along X and Y axis. Right, Stacked bar plots showing the proportion of Fibroblasts. P values by Mann-Kendall trend test. (i) EMT-*early* and corresponding ligands in situ distribution. (j) Co-localization of $ITGB4^{+}$/$ITGA3^{+}$EMT-*early* with their autocrine ligands.

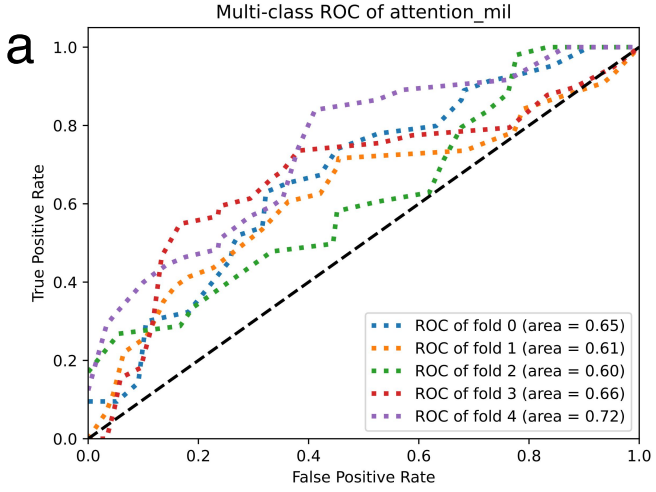
a
Multi-class ROC of attention_mil
True Positive Rate
False Positive Rate
ROC of fold 0 (area = 0.65)
ROC of fold 1 (area = 0.61)
ROC of fold 2 (area = 0.60)
ROC of fold 3 (area = 0.66)
ROC of fold 4 (area = 0.72)

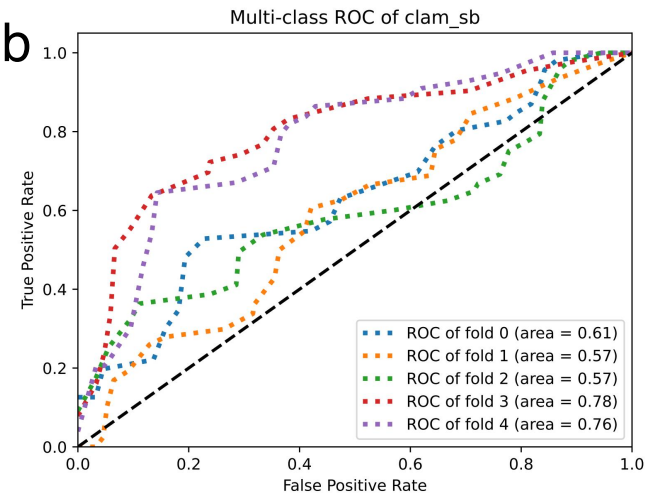
b
Multi-class ROC of clam_sb
True Positive Rate
False Positive Rate
ROC of fold 0 (area = 0.61)
ROC of fold 1 (area = 0.57)
ROC of fold 2 (area = 0.57)
ROC of fold 3 (area = 0.78)
ROC of fold 4 (area = 0.76)

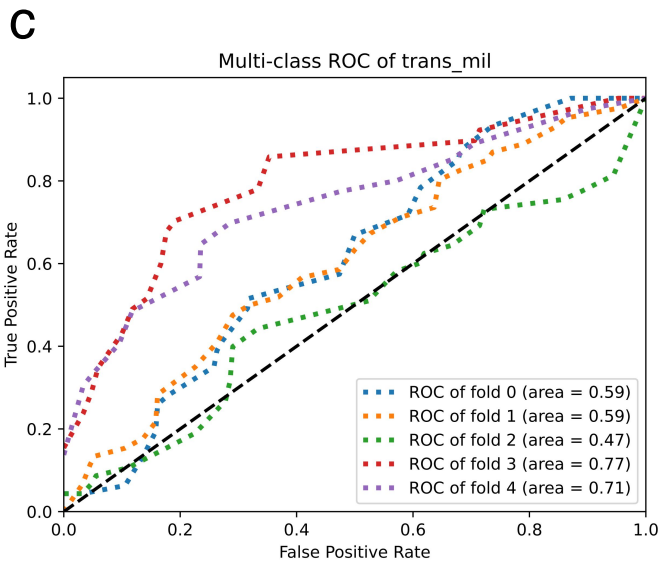
c
Multi-class ROC of trans_mil
True Positive Rate
False Positive Rate
ROC of fold 0 (area = 0.59)
ROC of fold 1 (area = 0.59)
ROC of fold 2 (area = 0.47)
ROC of fold 3 (area = 0.77)
ROC of fold 4 (area = 0.71)

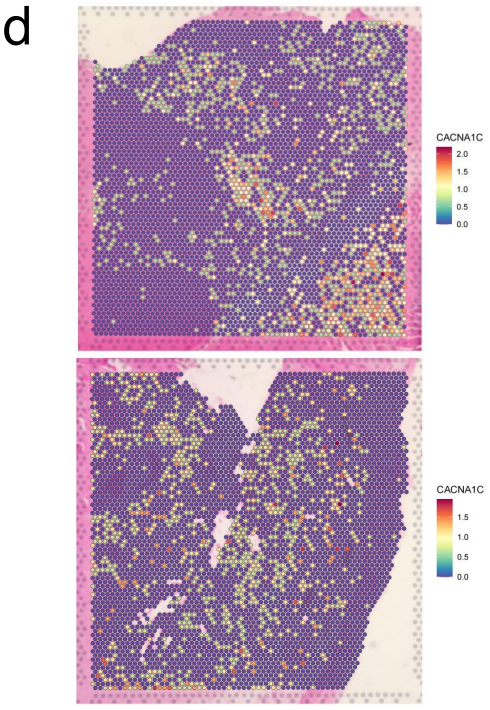
d
CACNA1C
CACNA1C

Figure S7. AMIL model performance evaluation.
(a-c) Five-fold cross-validation performance of the AMIL models. (d) In situ expression patterns of CACNA1C in Visium data.